Arabian Journal of Chemistry (2020) 13, 8361–8371

King Saud University

Arabian Journal of Chemistry

www.ksu.edu.sa
www.sciencedirect.com

ORIGINAL ARTICLE

Enhanced visible photocatalytic degradation of diclofen over N-doped TiO_2 assisted with H_2O_2: A kinetic and pathway study

Thang Phan Nguyen [a,b,1], Quoc Ba Tran [c,d,1], Quang Viet Ly [e,1], Le Thanh Hai [f], Duc Trung Le [f], Minh Bao Tran [f], Thi Thanh Tam Ho [g], Xuan Cuong Nguyen [c,d], Mohammadreza Shokouhimehr [h], Dai-Viet N. Vo [i], Su Shiung Lam [j], Huu-Tuan Do [k], Soo Young Kim [l,*], Tra Van Tung [f,*], Quyet Van Le [c,*]

[a] *Laboratory of Advanced Materials Chemistry, Advanced Institute of Materials Science, Ton Duc Thang University, Ho Chi Minh City, Vietnam*
[b] *Faculty of Applied Sciences, Ton Duc Thang University, Ho Chi Minh City, Vietnam*
[c] *Institute of Research and Development, Duy Tan University, Da Nang 550000, Vietnam*
[d] *Faculty of Environmental and Chemical Engineering, Duy Tan University, Da Nang 550000, Vietnam*
[e] *State Key Laboratory of Separation Membrane and Membrane Processes, National Center for International Joint Research on Membrane Science and Technology, School of Materials Science and Engineering, Tiangong University, Tianjin 300387, PR China*
[f] *Institute for Environment and Resource, Viet Nam National University Ho Chi Minh City, Ho Chi Minh 740500, Vietnam*
[g] *Department of Environment, An Giang University, An Giang, Vietnam*
[h] *Department of Materials Science and Engineering, Research Institute of Advanced Materials, Seoul National University, Seoul 08826, Republic of Korea*
[i] *Center of Excellence for Green Energy and Environmental Nanomaterials (CE@GrEEN), Nguyen Tat Thanh University, 300A Nguyen Tat Thanh, District 4, Ho Chi Minh City 755414, Vietnam*
[j] *Pyrolysis Technology Research Group, Institute of Tropical Aquaculture and Fisheries (AKUATROP) & Institute of Tropical Biodiversity and Sustainable Development (Bio-D Tropika), Universiti Malaysia Terengganu, 21030 Kuala Nerus, Terengganu, Malaysia*
[k] *Faculty of Environmental Sciences, VNU University of Science, Vietnam National University, Hanoi, 334 Nguyen Trai, Thanh Xuan, Hanoi, Vietnam*
[l] *Department of Materials Science and Engineering, Korea University, 145 Anam-ro, Seongbuk-gu, Seoul 02841, Republic of Korea*

Received 20 February 2020; accepted 16 May 2020
Available online 29 May 2020

* Corresponding authors.
E-mail addresses: nguyenphanthang@tdtu.edu.vn (T.P. Nguyen), sooyoungkim@korea.ac.kr (S.Y. Kim), travantung.moitruong@gmail.com (T. Van Tung), levanquyet@dtu.edu.vn (Q. Van Le).
[1] T. P. Nguyen, B. Q. Tran, Q. V. Ly contributed equally in this work.

Peer review under responsibility of King Saud University.

Production and hosting by Elsevier

https://doi.org/10.1016/j.arabjc.2020.05.023

KEYWORDS

Diclofenac;
Degradation;
Photocatalytic-membrane reactor;
N-doped TiO_2;
Visible photocatalysis

Abstract Increasing discharge and inadequate removal of pharmaceutical compounds pose significant concerns over global aquatic systems and human health. The accomplishment of affordable and safe water requires a stringent elimination of these micropollutants. This study evaluated the performance of Visible/N-doped TiO_2 and Visible/N-doped TiO_2/H_2O_2 processes using a submerged photocatalytic membrane reactor (SMPR) with suspended N-doped TiO_2 to address the removal of diclofenac (DCF). The kinetic and pathway of photodegradation of DCF were of particular interest in this study. The initial DCF concentrations upon the experiments were also examined using a wide range of 5–50 mg/L and 20–100 mg L^{-1} for Vis/N-doped TiO_2, and Vis/N-doped TiO_2/H_2O_2 process, respectively. The results indicated that higher initial concentration reduces the efficiency of the process, but one with H_2O_2 demonstrated an enhanced performance. The experimental data were found to fit well a pseudo-first-order kinetic model. Our findings demonstrated the analogous pathways of DCF for both processes. The Vis/N-doped TiO_2/H_2O_2 process tends to hasten the degradation rate as evidenced by the disappearance of some DCF byproducts at a similar irradiation period as compared to the other. The study provided useful information of the degradation rate and the potential formation of DCF intermediates upon the hybrid photocatalytic systems, therefore being of importance for scaling-up as well as evaluating potential detoxification of DCF upon the novel photocatalytic system.

1. Introduction

Over the past few decades, growing attention has been paid to pharmaceutical products as emerging environmental pollutants (Wang et al., 2016). These micropollutants could be widely encountered in many types of water resources largely through hospital- and household-generated wastewaters, and from pharmaceutical industrial effluents (Boleda et al., 2011). Most of the conventional designed wastewater treatment plants (WWTPs) are not sufficient to tackle pharmaceuticals due to their persistence and outstanding structural stability, consequently leading to their increasing presence in the aquatic systems. As a result, they not only pose great threats to aquatic organisms but also could potentially risk human health (Boleda et al., 2011; Wang et al., 2016).

Diclofenac (DCF) is a synthetic non-steroidal anti-inflammatory drug widely used to treat inflammatory and painful diseases of rheumatic and non-rheumatic origin (Calza et al., 2006). It is a recalcitrant organic pollutant that is hardly biodegradable, and thus difficult to completely remove by conventional wastewater treatment processes. The extensive use of DCF in European (EU) countries results in the dominant presence of this pharmaceutical in many WWTPs with the concentration range of 0.14–1.6 μm L^{-1} (Zhang et al., 2008). Literature reported that the percentage removal of DCF could vary a wide range, with an average of around 21–40% in WWTP effluents (Ternes, 1998). As a result, the DCF concentration was also detected in some estuaries with a range of 0.006–0.195 mg L^{-1} (Thomas and Hilton, 2004) and in rivers and lakes with a range of 0.024–0.500 mg L^{-1} (Zhang et al., 2008). DCF has reportedly limited acute toxicity on bacteria, algae, microcrustaceans, and fishes, but could pose severe harmful effects on aquatic organisms regarding chronic exposure (Ferrari et al., 2003). Earlier studies witnessed the damage of the kidneys and gills of fish once being exposed to DCF. Besides, the bioaccumulation of DCF was also observed in the fish tissues (Triebskorn et al., 2004). According to Hernando and coworkers, EC_{50} of DCF for bacteria was less than 1 mg/L, while that for vertebrates and algae occurred at a much higher concentration i.e., 1–10 mg/L (Hernando et al., 2006).

Photocatalysis has emerged as a foremost reliable application with high efficiency for the pharmaceutical degradation (Dong et al., 2019; Li et al., 2019, 2020; Sarasidis et al., 2014; Truong et al., 2019) due to its benefits of good photocatalytic activity, nontoxicity, chemical inertness, and low cost (Buscio et al., 2015). Many different photocatalysts have been developed recently for various applications such as perovskites (Huynh et al., 2020; Park et al., 2018), graphitic carbon nitride (Lam et al., 2020), transition metal oxides (Do et al., 2020; Nguyen et al., 2020a), transition metal carbides (Nguyen et al., 2020b, 2020c) and transition metal sulfides (Hasani et al., 2019a, 2019b; Tekalgne et al., 2019). Among those, TiO_2 is the most promising photocatalyst for wastewater treatment because of its high photocatalytic activity, stability low cost, and safety for humans and environment (Ata et al., 2017, Lee and Park, 2013). However, TiO_2 (pure anatase) particles mainly absorb ultraviolet light which accounts for 3–5% from solar energy. However, TiO_2 doping with non-metals (N, C, and S) or metals (Cu, Fe, Ag, Cr, Pt, Pd, Rh, Ir, Os, and Au) can absorb the visible light (400–700 nm). Doping of metal/no-metal atoms into TiO_2 also increases its conductivity (Sahasrabudhe et al., 2016). Notably, N is more effective than other dopants (C, S, P) in narrowing the optical bandgap of TiO_2 because of closing energy between N 2p state and O 2p state (Ansari et al., 2016).

Another concept is to pair photocatalytic processes with hydroxyl peroxide (H_2O_2) to enhance organic removal efficiency since it also offers several merits, including the forming of more hydroxyl radicals, preventing holes and electron recombination, and enhancement TiO_2 adsorption light (Achilleos et al., 2010; Irmak et al., 2004; Zou and Gao, 2011). So far, limited works have been carried out to examine the kinetics and decomposition pathways of DCF

by photocatalytic processes with and without H_2O_2 under visible irradiation using SMPR. Furthermore, the TiO_2 is a wide bandgap semiconductor (3–3.2 eV), which can only absorb light in the UV region, limiting its application in most of the photocatalytic systems (Chen and Selloni, 2014). To tackle these problems, doping strategies have been developed to enlarge the photocatalytic activity of TiO_2 under visible light (Fagan et al., 2016). Among those, N-doped TiO_2 was highly considered due to its high photocatalytic activity and can be manufactured at a relatively low-cost compared to other dopants such as Au, Ag, Pd, and Pt (Gomes et al., 2019).

Herein, we investigated the performance of SMPR with N doped-TiO_2 suspended nanoparticles (NPs) in the photoreactor under the photocatalytic process. This experiment also includes the influences of H_2O_2 regarding DCF photooxidation to provide an in-depth understanding of kinetics and the DCF degradation pathway along with proposing the possible mechanisms. The yield decomposition of DCF, determination of rate constants, and DCF byproducts during 180 min reaction time were also of interest.

2. Materials and methods

2.1. Chemicals and reagents

Commercial powder TiO_2 (Degussa-P25) (99.0%) and titanium tetraisopropoxide (TTiP) (97.0%) were supplied from Sigma Aldrich Co. Ltd, whereas diethanolamine (DEA) (98.5%) was obtained from Acros Organic, USA. Acetic acid (99.7%), hydrogen peroxide (30%), sodium hydroxide and sulfuric acid (96%) were purchased from Merck chemicals, Germany. Potassium iodide (99.5%) and ammonium nitrate (90%) were obtained from QRëC. Ammonium molybdate (81.0%), starch, and sodium thiosulfate (99.5%) were purchased from Ajax Finechem Pty Ltd. Ammonium hydroxide (NH_4^+, 28–30%) was supplied by Avantor. Diclofenac or DCF was purchased from Volnac, T.O. Pharma, Co. Ltd, Thailand. All chemicals were of analytical grade and used as received. Microfiltration (MF) membrane was obtained from Shandong Co, Ltd, China. MF ceramic membrane was made by alumina with a pore size of 50 nm, a pressure strength of 1.0 MPa, and an effective area of 0.0148 m^2. The visible fluorescent lamps, 50 W were purchased from Panasonic Co, Ltd, Thailand.

2.2. Preparation of N doped TiO_2

The sol-gel method was applied to synthesize N-doped TiO_2 NPs. Firstly, a certain amount of TTiP i.e., 4.5 mL was added into a beaker containing 15 mL acetic acid under a thoroughly stirring condition. Then, 30 mL of chili extract was added to the homogeneous solution. 2.5 mL DEA was subsequently added dropwise in the solution followed by a mild agitation for 30 min. The resultant solution was transferred into a ceramic dish and kept in a hood for drying over 24 h at room temperature. The sample was further dried at 100 °C in an oven for 2 h prior to further be calcinated at 500 °C at 30 min with the temperature increasing rate at 1 °C per min. Finally, the nascent powder was washed with ethanol and DI water for five times and dried in an oven at 105 °C for 2 h to obtain the desired N-doped TiO_2 NPs.

2.3. Experimental set up

The SMPR set up containing suspended N-doped TiO_2 under visible irradiation was applied to address synthetic wastewater containing DCF. SMPR was designed by a photoreactor cylindrical tank with an immersed tube MF ceramic membrane being at the center of the reactor. The membrane was connected to a suction pump to collect the water sample (Fig. 1). The photoreactor cylindrical tank was made by transparent glass with a working volume of 2 L. Five visible lamps with a power 50 W (420–720 nm) were installed outside and around the reactor.

The photocatalytic reactor was placed in a chamber. A magnetic stirrer was used to ensure uniformity of DCF molecules and catalyst suspension. Oxygen was continuously supplied through the pipe placed under the bottom of the UF membrane. The SMPR was conducted using the synthesized N-doped TiO_2 under visible light is denoted as "Vis/N-doped TiO_2" and that with H_2O_2 addition to the reaction is referred to "Vis/N-doped TiO_2/H_2O_2". The SMPR under Vis/N-doped TiO_2 and Vis/N-doped TiO_2/H_2O_2 processes were taken place for 180 min to investigate the DCF removal, kinetics, and pathways its products. Operating factors with different initial DCF concentrations were investigated for either scenario. To ensure uniformity of DCF molecules in solution was mixed by a magnetic stirrer. Oxygen was supplied though the pipe, placed under the bottom of MF membrane.

2.4. Analytical methods

The surface morphology of TiO_2 was examined using a scanning electron microscope (SEM) (JSM5600LV, Japan) and transmission electron microscopy (TEM, JEM-2100F, by JEOL). The finger-print functional groups of the N-doped TiO_2 NPs were assessed by the attenuated total reflectance Fourier transform-infrared (ATR-FTIR) spectrophotometer (PerkinElmer 100) with the scanning wavelength of 450–4000 1/cm. Prior to being measured, N-doped TiO_2 particles were shaped into pellets using potassium bromide. The pH point of zero charge of the N-doped TiO_2 NPs surface was determined by using Zeta sizer Nano ZS, Malvern Instruments Ltd, Malvern (UK).

The residual DCF concentrations were withdrawn from the reactor and measured by UV–Vis spectrophotometer (SENESYS 10S, Thermo Scientific) at wavelength 276 nm (Achilleos et al., 2010). Total organic carbon (TOC) was determined by TOC analyzer (TOC-L CPH, Shimadzu), operating in non-purge organic carbon mode with a relative precision of $< 5\%$. DCF products were analyzed by HPLC/MS/MS using Aligent 6200 series TOF/6500 series Q-TOF B.06.01 (B6172SP1) with the column ZORBAX Eclipse Plus (4.6 × 150 mm, 3,5 μm). The injection volume was 20 μL and a flow rate of 500 μL/min. Pathways of DCF under two modes i.e., Vis/N-doped TiO_2 and Vis/N-doped TiO_2/H_2O_2 were identified by measuring water sample at the interval time of 60 min.

To ensure that DCF degradation is entirely driven by the photocatalytic processes, the experiments of DCF exposed to hydroxyl peroxide (H_2O_2) in 3 h were investigated. The result showed that no direct H_2O_2 oxidation did take place for DCF. A slight decrease of DCF concentration, however, occurred

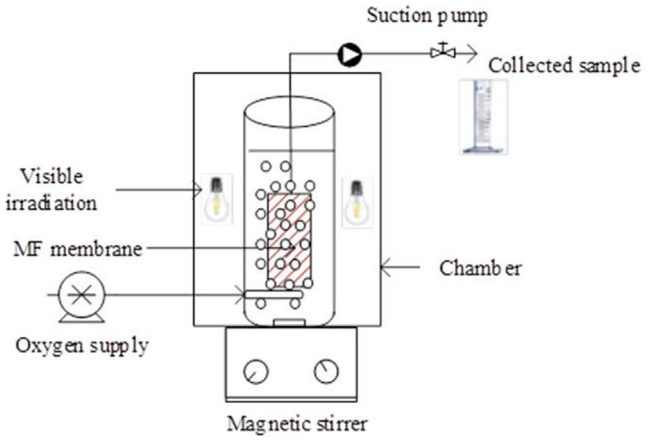

Fig. 1 Reactor set up.

under dark conditions, possibly due to its adsorption onto the N-doped TiO_2 particle surface. The adsorption reached equilibrium within 30 min prior to turning visible light on, therefore, confirming the adsorption steady state of DCF on the N-doped TiO_2 surface was reached.

3. Result and discussion

3.1. N-doped TiO_2 characteristics

The characteristics of N-doped TiO_2 were firstly confirmed by SEM, TEM and FTIR as shown in Fig. 2. The particle size of

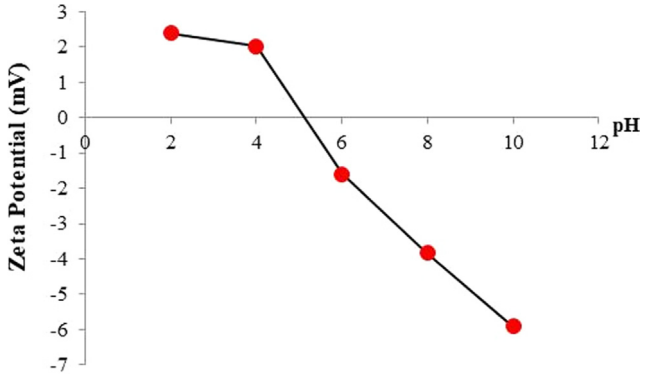

Fig. 3 Zeta potential profiles of N-doped TiO_2 as the function of pH.

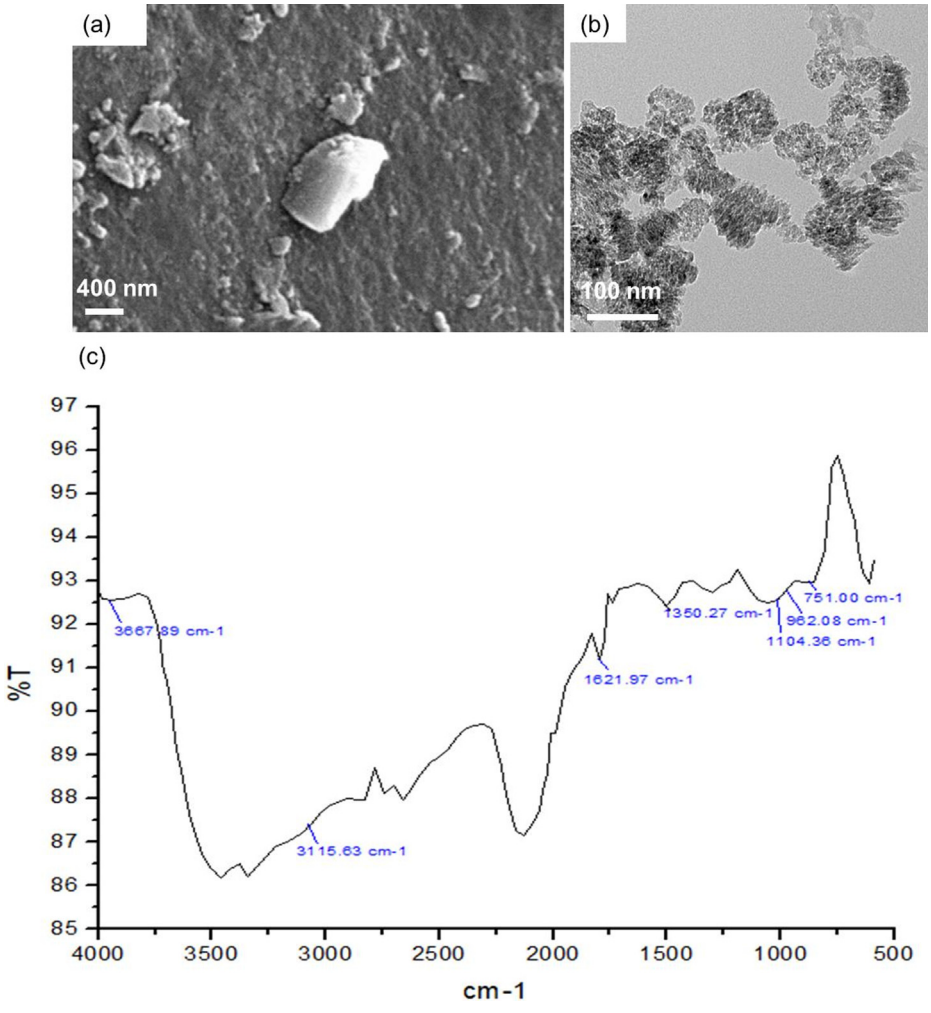

Fig. 2 (a) SEM top view image of N-doped TiO_2, (b) TEM image of N-doped TiO_2, (c) FTIR spectra of N doped TiO_2.

Table 1 Values of kinetic parameters for photodegradation of DCF by SMPR under Vis/N-doped TiO_2 and Vis/N-doped TiO_2/H_2O_2 processes.

DCF concentration (mg/L)	Vis/N-doped TiO_2			Vis/N-doped TiO_2/H_2O_2		
	r (mgL^{-1} min^{-1})	k_{obs} (min^{-1})	R^2	R (mgL^{-1} min^{-1})	k_{obs} (min^{-1})	R^2
5	0.0023	0.0068	0.9997	–	–	–
10	0.0022	0.0045	0.9987	0.0059	0.0088	0.9729
20	0.0021	0.0035	0.999	0.0028	0.0088	0.9988
50	0.0009	0.0010	0.9817	0.0014	0.0021	0.9929
100	–	–		0.0006	0.0007	0.9198

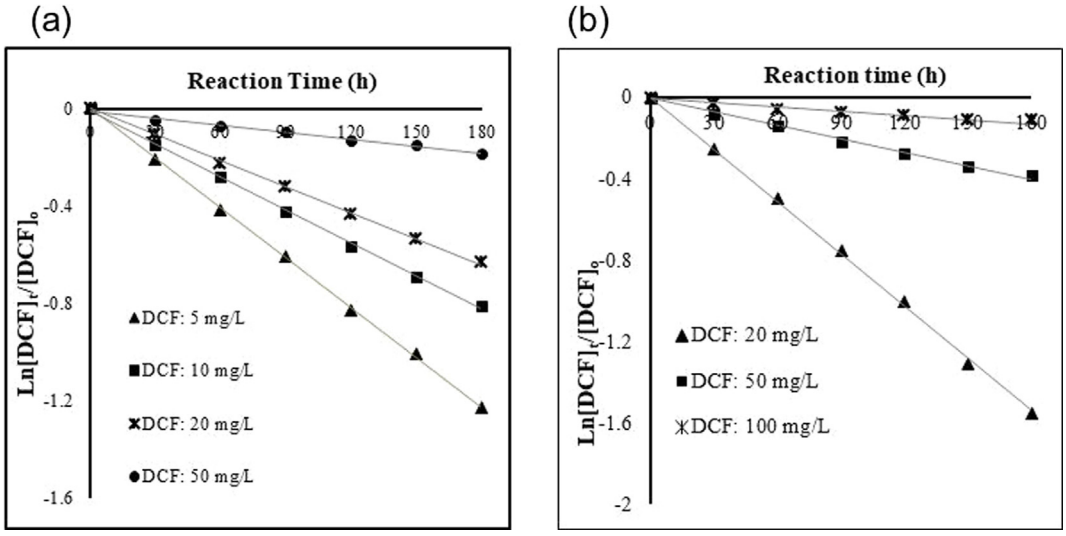

Fig. 4 Pseudo-first-order kinetic plot of DCF Photocatalytic oxidation under varying DCF initial concentration by SMPR with suspended N-doped TiO_2, (a) Vis/N-doped TiO_2 process and (b) Vis/N-doped TiO_2/H_2O_2 process.

N-doped TiO_2 was revealed to be 40–80 nm (Fig. 2a and b). The FTIR spectrum of N doped TiO_2 NPs was displayed in Fig. 2c. As can be seen, N-doped TiO_2 NPs exhibited the broad absorption band at around 3100–3500 cm^{-1}, with the peak appearing at around 3400 cm^{-1}, representing the stretching vibration of —OH groups. This was further corroborated by another peak shown at 1621 cm^{-1}. The specific Ti—O bending vibration could be seen at 750 cm^{-1}. The obvious peak at 1104–1350 cm^{-1} is affirmative for the N—H linkage, thus providing undeniable evidence for the successful formation of N-doped TiO_2 NPs (Cheng et al., 2016).

Fig. 3 demonstrated the changes zeta potential values of the N-doped TiO_2 upon different pH conditions. The pH_{pzc} value, which was determined based on the relationship between pH_f and pH_i, was constant regardless of KCl concentration, solid/liquid ratio, indicating that the absence of monovalent ions such as K, Cl on N-doped TiO_2 surface at the given pH magnitude. In this study, the pH_{pzc} was at the pH value of approximately 5, demonstrating that if the pH of the solution is larger than pH_{pzc} the NPs likely exhibit positive charge and vice versa. Generally, the point zero charge of TiO2 range from pH of 5–6.6 (Kosmulski, 2002). The pH_{pzc} (N-TiO_2) of this study was around 5. In the N-TiO_2 particles, nitrogen atoms were substitutionaly introduced into oxygen sites of TiO_2 lattice. Thus, the pH_{pzc} of N-TiO_2 was lower than PZC of TiO_2.

3.2. Kinetic of photooxidation of DCF under batch conditions of SMPR

It is well recognized that the kinetic rate of a given compound during a specific chemical process is largely governed by its initial concentration (Ito et al., 2005). In this study, the effects of the initial concentration on the kinetic information of DCF under photocatalytic reduction in two separate SMPR systems i.e., Vis/N-doped TiO_2 and Vis/N-doped TiO_2/H_2O_2 were examined using the different initial concentrations of DCF varying from 5 to 50, and 20–100 mg L^{-1} for Vis/N-doped TiO_2 and Vis/N-doped TiO_2/H_2O_2 processes, respectively. Other parameters such as pH, N-doped TiO_2 concentration and H_2O_2 concentration were kept fixed at the values of 6.5, 1 g L^{-1} and 15 mM, respectively. These given values were proven as the best operating condition for DCF removal efficiency by SMPR under visible irradiation (the results are not shown). The removal rate of DCF upon Vis/N-doped TiO_2 and Vis/N-doped TiO_2/H_2O_2 processes at different initial concentrations during 3 h of experiments were illustrated in Fig. 8a. As can be observed, DFC was effectively eliminated in either hybrid photocatalytic processes. This phenomenon was attributable to the capability of N-doped TiO_2 particles to absorb visible light to produce hydroxyl radicals (OH·) (Ananpattarachai et al., 2016), which can play an essential role in the degradation of DCF. The photocatalytic Vis/N-doped TiO_2 process with

the addition of H_2O_2 could impose enhanced DCF removal efficiency compared to that without H_2O_2 (Fig. 8b), as evidenced by the steeper slope of $Ln([DCF_t]/[DCF_o])$ of the former. It is due to the strong oxidation properties of H_2O_2 that can scavenge excited electrons of TiO_2 particles and conduction bands to generate hydroxyl radical and hydroxyl anion (Eq. (1) and (2)) (Velegraki et al., 2006). As a result, this phenomenon prevents the recombination of the electron (e^-) and hole (h^+) (Achilleos et al., 2010), increasing the hydroxyl radical and h^+ to react with DCF molecular. In addition, H_2O_2 can react with oxygen species to produce more hydroxyl radicals (Eq. (3)) (Irmak et al., 2004). Moreover, H_2O_2 adsorbs on TiO_2 nanoparticles to form peroxo complexes between H_2O_2 and Ti^{4+} ion that increases the adsorption capacity of TiO_2 under visible irradiation (Zou and Gao, 2011). As a result, more hydroxyl radicals (OH.) were formed that leads to increasing DCF oxidation of hydroxyl radicals.

$$TiO_2\ (e^-) + H_2O_2 \rightarrow TiO_2\ (h^+) + {\cdot}OH + OH^- \quad (1)$$

$$H_2O_2 + e^-{}_{CB} \rightarrow {\cdot}OH + OH^- \quad (2)$$

$$H_2O_2 + {\cdot}O^-{}_2 \rightarrow {\cdot}OH + OH^- + O_2 \quad (3)$$

Numerous researches working on heterogeneous photocatalysis reported that the Langmuir-Hinshelwood kinetic model (Eq. (4)) fitted well with the mineralization rate of various organic contaminants over illuminated TiO_2 photocatalytic oxidation. This kinetic model of use to quantify the kinetic rate of the photocatalysis among two separated photocatalytic systems was based on the following equation:

$$r = \frac{k_r K C_s}{1 + K C_s} \quad (4)$$

where r is reaction rate, C_s is reactant concentration on the catalyst surface (mol/m^3) in equilibrium with the bulk concentration, k_r is the reaction rate constant ($mol/m^3/s$), and K represents adsorption–desorption equilibrium constant (m^3/mol).

The kinetic constants (k_{obs}) were calculated from the pseudo-first-order equation (Eq. (5)).

$$Ln\frac{[DCF]_{T,t}}{[DCF]_{T,o}} = -k_{obs}t \quad (5)$$

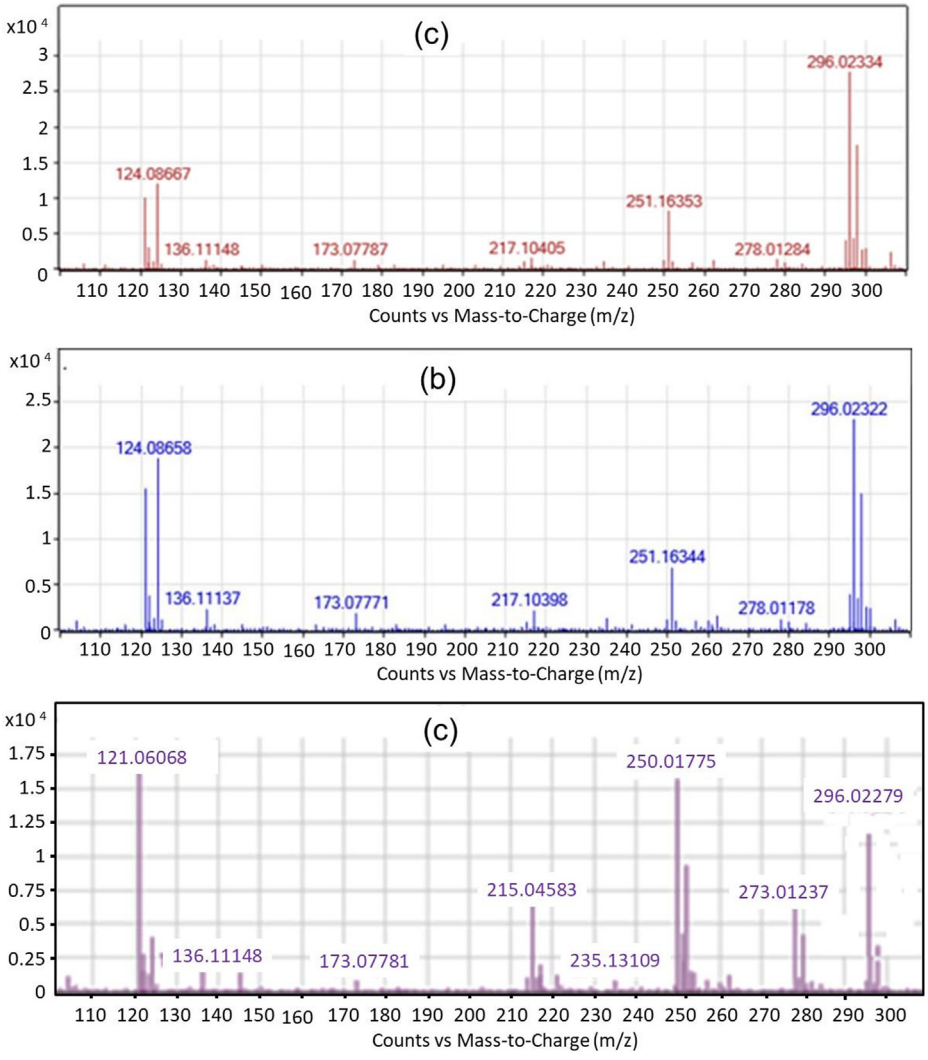

Fig. 5 HPLC/MS/MS data showing the presence of DCF product degradation from the Vis/N-doped TiO_2 process; (a) mass chromatogram at 60 min; (b) at 120 min; (c) and at 180 min.

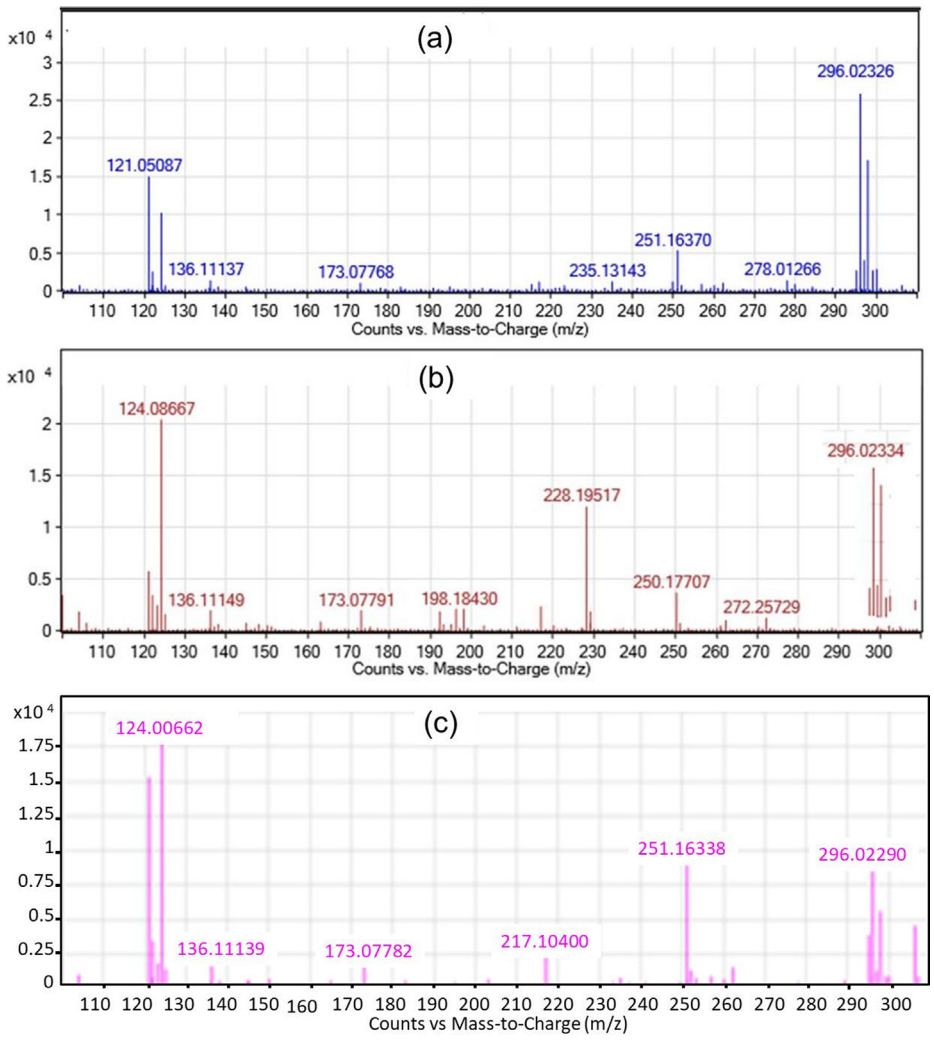

Fig. 6 HPLC/MS/MS data showing the presence of DCF product degradation from the Vis/N-doped TiO_2/H_2O_2 process; (a) mass chromatogram at 60 min; (b) at 120 min; (c) and at 180 min.

where k_{obs} is pseudo-first-order kinetic constant, $[DCF]_{T,o}$ is the total initial concentration of DCF, and $[DCF]_{T,t}$ is DCF concentration at t time. For each experiment, k_{obs} was determined from the slope of the linear time course plot of Ln $([DCF]_{T,t}/[DCF]_{T,o})$.

At low initial concentration, our data showed a strong correlation with the Langmuir-Hinshelwood model for both processes (Vis/N-doped TiO_2 and Vis/N-doped TiO_2/H_2O_2). However, the correlation i.e., R^2 tended to decrease at the concentration of 100 mg/L (Table 1). The plots of $Ln([DCF]_t/[DCF]_o)$ of DCF concentrations versus time for either process exhibited the straight linear, of which the slopes upon linear regression equations represented first-order rate constant k_{obs} first-order kinetic (Fig. 4a-b). The reaction rates (r) and kinetic constants of different DCF concentrations from both the photocatalytic process with and without H_2O_2 are shown in Table 1. Results indicated that the reaction rates were consistently reduced with the increasing DCF concentration regardless of photodegradation processes. For instance, the photodegradation rate of Vis/N-doped TiO_2 systems continuously dropped from 0.0023 to 0.0009 mg L^{-1} min^{-1} as the initial concentration of DCF increase from 5 to 50 mg L^{-1}. Table 1 indicated a quantitative proof for the enhancement of the photodegradation process upon the addition of H_2O_2. Considering the similar range of the initial concentration from 20 to 50 mg L^{-1}, Table 1 demonstrated that the mineralization rate of DCF in Vis/N-doped TiO_2 increased for around two times, relatively lower than that in Vis/N-doped TiO_2/H_2O_2 i.e., more than three times.

3.3. Fate of the DCF decomposition byproducts under visible irradiation photocatalytic processes

The water samples were withdrawn at each irradiation period i.e., 60, 120, and 180 min for the analysis of the DCF products by HPLC/MS/MS. The experiments were set up at the optimal operational condition as described in Section 3.2, with the initial concentration of DCF being 20 mg L^{-1}. Compared to the original chemical structure, the results indicated that DCF was degraded into many different byproducts under the photocatalytic oxidation processes. The *m/z* chromatogram representative of DCF byproducts upon Vis/N-doped TiO_2

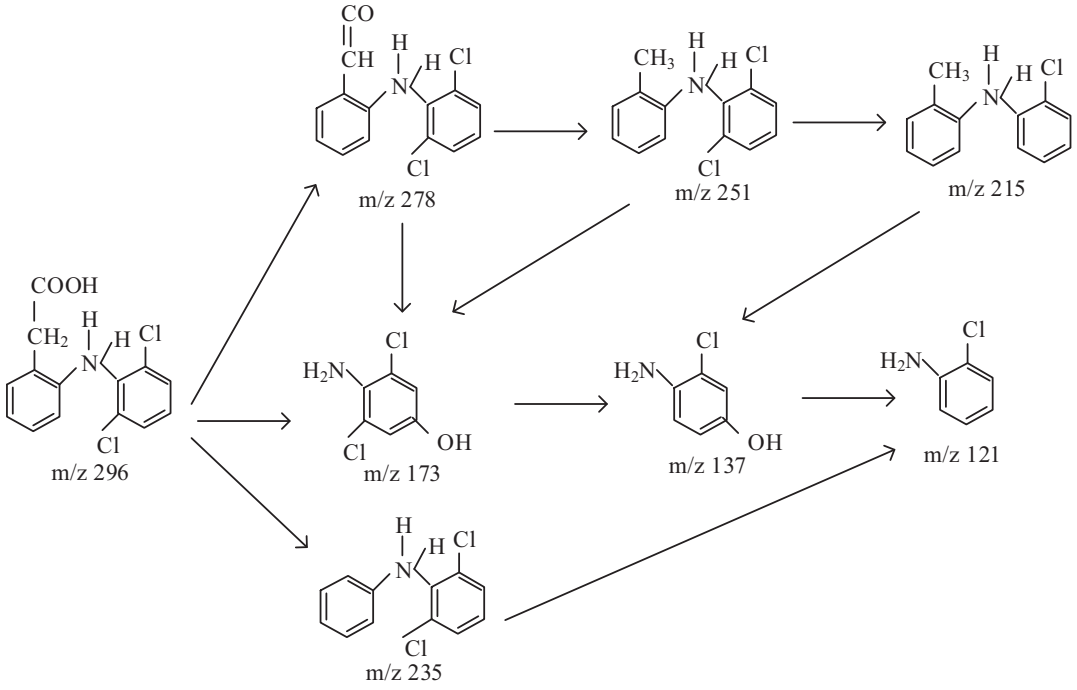

Fig. 7 The proposed photocatalytic mechanism for DCF degradation under Vis/N-doped TiO_2 process.

and Vis/N-doped TiO_2/H_2O_2 were depicted in Figs. 5 and 6, respectively. The structural assignments of all detected product breakdowns were based on analysis of the m/z molecular ions peaks comparable to the standard ones. DCF and TOC removal efficiency at the end of the reaction were 42.21 and 16.41%, respectively for Vis/N-doped TiO_2 process and 79.55 and 30.47% for Vis/N-doped TiO_2/H_2O_2 process, respectively.

Based on the corresponding fragmentation patterns as well as the DCF and TOC results, the degradation pathway of the given micropollutants was suggested, as shown in Figs. 7 and 8 for Vis/N-doped TiO_2 and Vis/N-doped TiO_2/H_2O_2, respectively. Not only the similar degradation pathway but similar byproducts formation were observed in either process. Firstly, Figs. 7 and 8 suggested that either process could release the hydroxyl group of the DCF to form a fragment at m/z of 278 g mol^{-1}, which could further lose formic acid group producing another fragment at m/z of 251 g mol^{-1}. This secondary byproduct could form the tertiary chemical compound associated with m/z of 215 g/mol by losing formic acid and chlorine radical (Calza et al., 2006), decomposing the pristine DCF i.e., m/z of 296 g mol^{-1}. The second degradation route resulted in a fragment at m/z 173 g mol^{-1}, which indicates that the cleavage of the C-N bond of DCF was split into two parts by hydroxyl radical attack (Banaschik et al., 2018). The formation of 2, 6-dichlorophenol and 4-chlorocathecol are formed in one direction, while cathecol and hydroquinone are formed by another (Michael et al., 2014). The ion at m/z 137 g/mol produced a fragment at m/z 121 g mol^{-1}, though the loss of chlorine radical, and loses the lateral chain (Banaschik et al., 2018). The third route of DCF decomposition is to produce a chemical fragment at m/z 235 g mol^{-1} by releasing the carboxyl group (COOH).

However, the results indicated that some DCF products were slightly different among the two processes (Vis/N-doped TiO_2 and Vis/N-doped TiO_2/H_2O_2). For example, in Vis/N-doped TiO_2 process (Fig. 5), a fragment with m/z of 235 g mol^{-1} at the reaction time of 180 min was observed while that was only appeared at a reaction time of 60 min, and the peaks associated with the fragment was then disappeared at a longer irradiation under Vis/N-doped TiO_2/H_2O_2 process (Fig. 6). Other DCF products linked with m/z of 198 and 228 g mol^{-1} were formed at 120 min under the Vis/N-doped TiO_2/H_2O_2 process and disappeared at 180 min (Fig. 6), but these products were not found in the Vis/N-doped TiO_2 process. Besides, the former was shown to introduce some unique chemical formulas associated with m/z of 228 and 198 g mol^{-1} by releasing two chlorine ions and forming the aldehyde group. The result indicated that when reactive hydroxyl radicals (·OH) in the Vis/N-doped TiO_2/H_2O_2 process was dominant, hydroxyl radicals easily reacted with DCF to form aldehyde group and released chlorine ions. As a result, the small molecules from the DCF photocatalytic oxidation from the Vis/N-doped TiO_2 process were, 278, 251, 235, 215, 173, 137 and 121 g mol^{-1}, and from the Vis/N-doped TiO_2/H_2O_2 process, were 278, 251, 235, 228, 215, 198, 173, 137 and 121 g mol^{-1} (Figs. 5 and 6).

4. Conclusion

The study provides insights into the kinetic rate and degradation pathways of the DCF micropollutants by photocatalytic oxidation upon with and without H_2O_2. Results showed that N-doped TiO_2 absorbed visible light for DCF degradation, and the addition of H_2O_2 with the Vis/N-doped TiO_2 photocatalytic process enhanced the DCF removal efficiency. The degradation of DCF from both processes fitted well with the pseudo-first-order kinetics. In addition, HPLC/MS/MS results indicated that DCF degradation was found to follow the

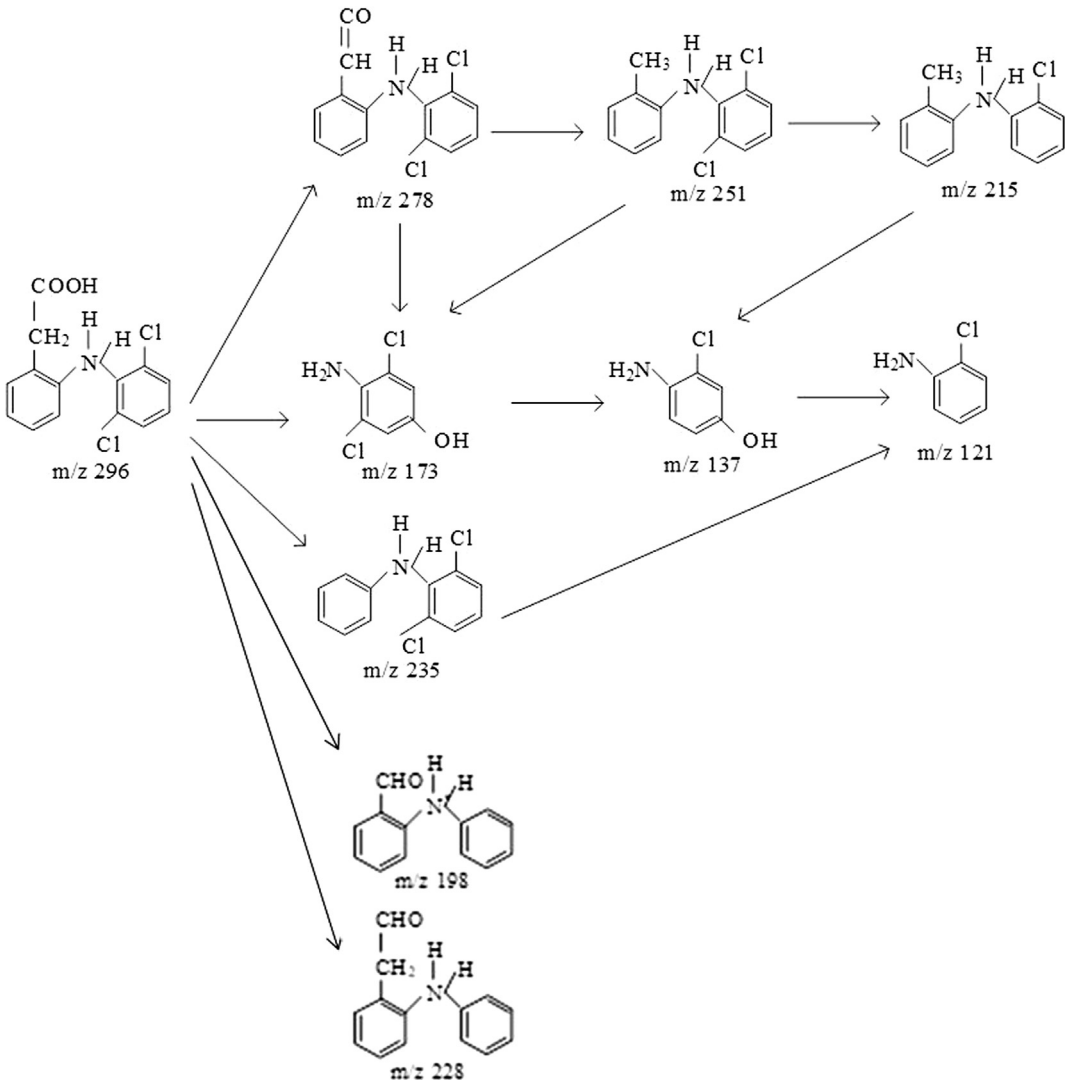

Fig. 8 The proposed photocatalytic mechanism for DCF degradation from the Vis/N-doped TiO_2/H_2O_2 process.

photocatalytic pathways leading to the intermediates of parent pharmaceuticals, C—N bonding cleavage intermediates of red-oxidation radicals of the photocatalytic process, and direct decarboxylation, subsequently, the dechlorination and oxidation products decrease via competitive routs. The study sheds light on proposing the tentative mechanism of DCF degradation under different photocatalytic processes i.e., with and without H_2O_2, and further works should be carried out to warrant the successful full-scale hybrid systems application for the DCF as well as other recalcitrant micropollutants.

Declaration of Competing Interest

The authors declare that they have no known competing financial interests or personal relationships that could have appeared to influence the work reported in this paper.

Acknowledgments

The research team would like to thank the Vietnam National University in Ho Chi Minh City (VNU-HCM) for funding the research project KHCN-TNB.ĐT/14-19/C25. This research was also partly supported by the Creative Materials Discovery Program through the NRF funded by Ministry of Science and ICT [grant number 2017M3D1A1039379] and the Basic Research Laboratory of the NRF funded by the Korean government [grant number 2018R1A4A1022647].

References

Achilleos, A., Hapeshi, E., Xekoukoulotakis, N.P., Mantzavinos, D., Fatta-Kassinos, D., 2010. Factors affecting diclofenac decomposition in water by UV-A/TiO2 photocatalysis. Chem. Eng. J. 161 (1), 53–59.

Ansari, S.A., Khan, M.M., Ansari, M.O., Cho, M.H., 2016. Nitrogen-doped titanium dioxide (N-doped TiO2) for visible light photocatalysis. New J. Chem. 40 (4), 3000–3009.

Ata, R., Sacco, O., Vaiano, V., Rizzo, L., Tore, G.Y., Sannino, D., 2017. Visible light active N-doped TiO2 immobilized on polystyrene as efficient system for wastewater treatment. J. Photochem. Photobiol. A 348, 255–262.

Banaschik, R., Jablonowski, H., Bednarski, P.J., Kolb, J.F., 2018. Degradation and intermediates of diclofenac as instructive example

for decomposition of recalcitrant pharmaceuticals by hydroxyl radicals generated with pulsed corona plasma in water. J. Hazard. Mater. 342, 651–660.
Boleda, M.R., Galceran, M.T., Ventura, F., 2011. Behavior of pharmaceuticals and drugs of abuse in a drinking water treatment plant (DWTP) using combined conventional and ultrafiltration and reverse osmosis (UF/RO) treatments. Environ. Pollut. 159 (6), 1584–1591.
Buscio, V., Brosillon, S., Mendret, J., Crespi, M., Gutiérrez-Bouzán, C., 2015. Photocatalytic membrane reactor for the removal of C.I. Disperse Red 73. Materials 8 (6), 3633–3647.
Calza, P., Sakkas, V.A., Medana, C., Baiocchi, C., Dimou, A., Pelizzetti, E., Albanis, T., 2006. Photocatalytic degradation study of diclofenac over aqueous TiO2 suspensions. Appl. Catal. B 67 (3), 197–205.
Chen, X., Selloni, A., 2014. Introduction: titanium dioxide (TiO2) nanomaterials. Chem. Rev. 114 (19), 9281–9282.
Cheng, X., Yu, X., Xing, Z., Yang, L., 2016. Synthesis and characterization of N-doped TiO2 and its enhanced visible-light photocatalytic activity. Arabian J. Chem. 9, S1706–S1711.
Do, H.H., Nguyen, D.L.T., Nguyen, X.C., Le, T.-H., Nguyen, T.P., Trinh, Q.T., Ahn, S.H., Vo, D.-V.N., Kim, S.Y., Le, Q.V., 2020. Recent progress in TiO2-based photocatalysts for hydrogen evolution reaction: A review. Arabian J. Chem. 13 (2), 3653–3671.
Dong, X.a., Cui, W., Wang, H., Li, J., Sun, Y., Wang, H., Zhang, Y., Huang, H., Dong, F., 2019. Promoting ring-opening efficiency for suppressing toxic intermediates during photocatalytic toluene degradation via surface oxygen vacancies. Sci. Bull. 64 (10), 669–678.
Fagan, R., McCormack, D.E., Dionysiou, D.D., Pillai, S.C., 2016. A review of solar and visible light active TiO2 photocatalysis for treating bacteria, cyanotoxins and contaminants of emerging concern. Mater. Sci. Semicond. Process. 42, 2–14.
Ferrari, B.t., Paxéus, N., Giudice, R.L., Pollio, A., Garric, J., 2003. Ecotoxicological impact of pharmaceuticals found in treated wastewaters: study of carbamazepine, clofibric acid, and diclofenac, Ecotoxicol. Environ. Saf. 55 (3), 359–370.
Gomes, J., Lincho, J., Domingues, E., Quinta-Ferreira, R.M., Martins, R.C., 2019. N-TiO2 photocatalysts: a review of their characteristics and capacity for emerging contaminants removal. Water 11 (2), 373.
Hasani, A., Le, Q.V., Tekalgne, M., Choi, M.-J., Lee, T.H., Jang, H. W., Kim, S.Y., 2019a. Direct synthesis of two-dimensional MoS2 on p-type Si and application to solar hydrogen production. NPG Asia Mater. 11 (1), 47.
Hasani, A., Van Le, Q., Tekalgne, M., Choi, M.-J., Choi, S., Lee, T. H., Kim, H., Ahn, S.H., Jang, H.W., Kim, S.Y., 2019b. Fabrication of a WS2/p-Si heterostructure photocathode using direct hybrid thermolysis. ACS Appl. Mater. Interfaces 11 (33), 29910–29916.
Hernando, M.D., Mezcua, M., Fernández-Alba, A.R., Barceló, D., 2006. Environmental risk assessment of pharmaceutical residues in wastewater effluents, surface waters and sediments. Talanta 69 (2), 334–342.
Huynh, K.A., Nguyen, D.L.T., Nguyen, V.-H., Vo, D.-V.N., Trinh, Q. T., Nguyen, T.P., Kim, S.Y., Le, Q.V., 2020. Halide perovskite photocatalysis: progress and perspectives. J. Chem. Technol. Biotechnol. https://doi.org/10.1002/jctb.6342.
Irmak, S., Kusvuran, E., Erbatur, O., 2004. Degradation of 4-chloro-2-methylphenol in aqueous solution by UV irradiation in the presence of titanium dioxide. Appl. Catal. B 54 (2), 85–91.
Ito, N., Suzuki, M., Kusai, A., Takayama, K., 2005. Effect of initial concentration on stability of panipenem in aqueous solution. Chem. Pharm. Bull. 53 (3), 323–327.
Ananpattarachai, Jirapat, Seraphin, Supapan, Kajitvichyanukul, P., 2016. Formation of hydroxyl radicals and kinetic study of 2-chlorophenol photocatalytic oxidation using C-doped TiO2, N-doped TiO2, and C, N Co-doped TiO2 under visible light. Environ. Sci. Pollut. Res. 23 (4), 3884–3896.
Kosmulski, M., 2002. The significance of the difference in the point of zero charge between rutile and anatase. Adv. Colloid Interface Sci. 99 (3), 255–264.
Lam, S.S., Nguyen, V.-H., Nguyen Dinh, M.T., Khieu, D.Q., La, D. D., Nguyen, H.T., Vo, D.-V.N., Xia, C., Shokouhimehr, M., Varma, R.S., Nguyen, C.C., Le, Q.V., Peng, W.-X., 2020. Mainstream avenues to boost graphitic carbon nitride efficiency: Toward enhanced solar-driven photocatalytic hydrogen production and environmental remediationJ. Chem. A Mater.
Lee, S.-Y., Park, S.-J., 2013. TiO2 photocatalyst for water treatment applications. J. Ind. Eng. Chem. 19 (6), 1761–1769.
Li, J., Dong, X.a., Zhang, G., Cui, W., Cen, W., Wu, Z., Lee, S.C., Dong, F., 2019. Probing ring-opening pathways for efficient photocatalytic toluene decomposition, J. Mater. Chem. A 7 (7), 3366–3374.
Li, J., Cui, W., Chen, P., Dong, X.a., Chu, Y., Sheng, J., Zhang, Y., Wang, Z., Dong, F., 2020. Unraveling the mechanism of binary channel reactions in photocatalytic formaldehyde decomposition for promoted mineralization, Appl. Catal. B 260, 118130.
Michael, I., Achilleos, A., Lambropoulou, D., Torrens, V.O., Pérez, S., Petrović, M., Barceló, D., Fatta-Kassinos, D., 2014. Proposed transformation pathway and evolution profile of diclofenac and ibuprofen transformation products during (sono)photocatalysis. Appl. Catal. B 147, 1015–1027.
Nguyen, T.P., Tuan Nguyen, D.M., Tran, D.L., Le, H.K., Vo, D.-V. N., Lam, S.S., Varma, R.S., Shokouhimehr, M., Nguyen, C.C., Le, Q.V., 2020a. MXenes: Applications in electrocatalytic, photocatalytic hydrogen evolution reaction and CO2 reduction. Molecular Catal. 486, 110850.
Nguyen, T.P., Nguyen, D.L.T., Nguyen, V.-H., Le, T.-H., Vo, D.-V. N., Trinh, Q.T., Bae, S.-R., Chae, S.Y., Kim, S.Y., Le, Q.V., 2020b. Recent advances in TiO2-based photocatalysts for reduction of CO2 to fuels. Nanomaterials 10 (2), 337.
Nguyen, V.-H., Nguyen, B.-S., Hu, C., Nguyen, C.C., Nguyen, D.L. T., Nguyen Dinh, M.T., Vo, D.-V.N., Trinh, Q.T., Shokouhimehr, M., Hasani, A., Kim, S.Y., Le, Q.V., 2020c. Novel Architecture Titanium Carbide (Ti3C2Tx) MXene cocatalysts toward photocatalytic hydrogen production: a mini-review. Nanomaterials 10 (4), 602.
Park, G.D., Lee, C.W., Nam, K.T., 2018. Recent advances and perspectives of halide perovskite photocatalyst. Curr. Opin. Electrochem. 11, 98–104.
Sahasrabudhe, G., Krizan, J., Bergman, S.L., Cava, R.J., Schwartz, J., 2016. Million-fold increase of the conductivity in TiO2 rutile through 3% niobium incorporation. Chem. Mater. 28 (11), 3630–3633.
Sarasidis, V.C., Plakas, K.V., Patsios, S.I., Karabelas, A.J., 2014. Investigation of diclofenac degradation in a continuous photocatalytic membrane reactor. Influence of operating parameters. Chem. Eng. J. 239, 299–311.
Tekalgne, M., Hasani, A., Le, Q.V., Nguyen, T.P., Choi, K.S., Lee, T. H., Jang, H.W., Luo, Z., Kim, S.Y., 2019. CdSe quantum dots doped WS2 nanoflowers for enhanced solar hydrogen production. Physica Status Solidi A Appl. Res. 216 (9), 1800853.
Ternes, T.A., 1998. Occurrence of drugs in German sewage treatment plants and rivers1Dedicated to Professor Dr. Klaus Haberer on the occasion of his 70th birthday.1. Water Res. 32 (11), 3245–3260.
Thomas, K.V., Hilton, M.J., 2004. The occurrence of selected human pharmaceutical compounds in UK estuaries. Mar. Pollut. Bull. 49 (5), 436–444.
Triebskorn, R., Casper, H., Heyd, A., Eikemper, R., Köhler, H.R., Schwaiger, J., 2004. Toxic effects of the non-steroidal anti-inflammatory drug diclofenac: Part II. Cytological effects in liver, kidney, gills and intestine of rainbow trout (Oncorhynchus mykiss). Aquat. Toxicol. 68 (2), 151–166.
Truong, H.B., Huy, B.T., Ly, Q.V., Lee, Y.-I., Hur, J., 2019. Visible light-activated degradation of natural organic matter (NOM) using zinc-bismuth oxides-graphitic carbon nitride (ZBO-CN) photocat-

alyst: Mechanistic insights from EEM-PARAFAC. Chemosphere 224, 597–606.

Velegraki, T., Poulios, I., Charalabaki, M., Kalogerakis, N., Samaras, P., Mantzavinos, D., 2006. Photocatalytic and sonolytic oxidation of acid orange 7 in aqueous solution. Appl. Catal. B 62 (1), 159–168.

Wang, Y., Ma, J., Zhu, J., Ye, N., Zhang, X., Huang, H., 2016. Multi-walled carbon nanotubes with selected properties for dynamic filtration of pharmaceuticals and personal care products. Water Res. 92, 104–112.

Zhang, Y., Geißen, S.-U., Gal, C., 2008. Carbamazepine and diclofenac: Removal in wastewater treatment plants and occurrence in water bodies. Chemosphere 73 (8), 1151–1161.

Zou, J., Gao, J., 2011. H2O2-sensitized TiO2/SiO2 composites with high photocatalytic activity under visible irradiation. J. Hazard. Mater. 185 (2), 710–716.